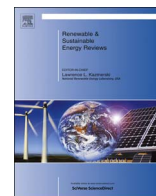




Contents lists available at ScienceDirect

Renewable and Sustainable Energy Reviews

journal homepage: www.elsevier.com/locate/rser

Review of techniques based on artificial neural networks for the electrical characterization of concentrator photovoltaic technology

Florencia Almonacid^{a,*}, Eduardo F. Fernandez^a, Adel Mellit^b, Soteris Kalogirou^c

^a Center for Advanced Studies in Energy and Environment (CEAEMA), University of Jaen, Campus Lagunillas, 23071 Jaen, Spain

^b Faculty of Sciences and Technology, Renewable Energy Laboratory, Jijel University, 18000, Algeria

^c Department of Mechanical Engineering and Materials Sciences and Engineering, Cyprus University of Technology, P.O. Box 50329, 3603 Limassol, Cyprus

ARTICLE INFO

Keywords:

Concentrator photovoltaics
Artificial neural networks
Electrical characterization

ABSTRACT

Concentrator photovoltaics (CPV) is considered to be one of the most promising renewable energy components that could lead to a reduction on the dependence on fossil fuels. The aim of CPV technology is to lower the cost of the system by reducing the semiconductor material, and replacing it by cheap optical devices that concentrate the light received from the sun on a small-size solar cell. The electrical characterization of devices based on this technology however, is inherently different and more complex than that of the traditional PV devices. Due to the advantages offered by the Artificial Neuron Networks (ANNs) to solve complex and non-linear problems, and the great level of complexity of electrical modelling of CPV devices, in recent years, several authors have applied a variety of ANNs to solve issues related to CPV technology. In this paper, a review of the ANNs developed to address various topics related with both, low and high concentrator photovoltaics, is presented. Moreover, a review of the ANN-based models to predict the main environmental parameters that affect the performance of CPV systems operating outdoors is also provided. Published papers presented show the potential of the ANNs as a powerful tool for modelling the CPV technology.

1. Introduction

Nowadays, photovoltaics (PV) are the most wide-spread solar energy system worldwide. Among the different PV technologies, concentrator photovoltaics (CPV) is considered as one of the most promising renewable energy system that could lead to a reduction on the dependence on fossil fuel [1,2]. The CPV systems are based on the use of cheap optical devices (lenses and mirrors) that concentrate the sunlight on a small-size solar cell. The aim of this technology is to lower the cost of the system by reducing the semiconductor material, which is the most expensive part in a PV system, so the costs of the electrical power generation can be reduced [3].

It is usual to classify the CPV systems according to the concentration ratio of the solar radiation incident onto the cell. This parameter gives the ratio between the lens area and the solar cell area. This ratio, as well as the optical efficiency of the system, indicates the number of times that the solar light is concentrated and is usually known as the number of 'Suns', which is equivalent to the number of times the sun power is multiplied. According to this ratio it is possible to classify the CPV systems into [4]:

- Low concentrator photovoltaics (LCPV) for systems with concentration ratio between 1 and 40 suns.
- Medium concentrator photovoltaics (MCPV) for systems with concentration ratio between 40 and 300 suns.
- High concentrator photovoltaics (HCPV) for systems with concentration ratio between 300 and 2000 suns.

Among these, the low concentration photovoltaic systems for building integration [5,6], and the high concentration photovoltaic systems for large scale implementation in big power plants [7,8], have shown the greatest potential for growth and development. Thus CPV and in particular LCPV and HCPV systems, could play an important role in the power generation markets in the coming years [9,10].

As in other type of PV technology, the prediction of the electrical characteristics of CPV systems is required for the design, monitoring, life cycle assessment, and therefore, for the accurate evaluation of the economic parameters to promote the market expansion of this emerging technology worldwide [11–14]. Moreover, the modelling of concentrator devices is inherently different and more complex than traditional PV technology [15,16]. The main concerns involved in the modelling of CPV technology are:

* Corresponding author.

E-mail address: facruz@ujaen.es (F. Almonacid).

<http://dx.doi.org/10.1016/j.rser.2016.11.075>

Received 22 February 2016; Received in revised form 3 October 2016; Accepted 1 November 2016

Available online xxx

1364-0321/© 2016 Elsevier Ltd. All rights reserved.

Nomenclature*Abbreviations*

AE	Absolute Error
AI	Artificial Intelligence
AM	Air Mass
ANFIS	Adaptive Neuro-Fuzzy Inference System
ANN	Artificial Neural Network
AOD	Aerosol optical depth
APE	Average Photon Energy
ARMSE	Absolute Root Mean Square Error
CPV	Concentrator Photovoltaics
DJ	Dual junction
E-ANN	Ensemble Artificial Neural Network
EQE	External Quantum Efficiency
FFNN	Feed-Forward back-propagation Neural Network
HCPV	High Concentrator Photovoltaic
LCPV	Low Concentrator Photovoltaics
MAE	Mean Absolute Error
MAPE	Mean Absolute Percentage Error
MCPV	Medium Concentrator Photovoltaics
MBE	Mean Bias Error
MJ	Multi Junction
MLR	Multiple Linear Regression
MLP	Multilayer Perceptron
MSE	Mean Square Error
MRE	Mean Relative Error
NRMSE	Normalised Root Mean Square Error
PV	Photovoltaics
RBF	Radial Basis Function Network
RCI	Reference Clearness Index
RMSE	Root Mean Square Error

SMR	Spectral Matching Ratio
TJ	Triple junction

Symbols units

λ	Wavelength nm
B	Irradiance W/m ²
d	Index of agreement
DI	Direct Normal Irradiance W/m ²
DNI	Direct Normal Irradiance W/m ²
DNI _c	Portion of the DNI transformed into heat W/m ²
DNI _{heat}	Portion of the DNI transformed into heat W/m ²
DHI	Diffuse Irradiance W/m ²
E _b (λ)	Spectral distribution of the DNI
f	Short circuit current A
GHI	Short circuit current A
I _{sc}	Short circuit current A
K _t	Clearness index
R ²	Correlation coefficient
S	Spectrum
SR(λ)	Spectral Response
P _{max}	Precipitable Water cm ²
PW	Precipitable Water cm ²
T	Temperature °C
T _{air}	Ambient Temperature °C
T _c	Heat-sink temperature °C
T _{h-s}	Heat-sink temperature °C
T _m	Module Temperature °C
V _{oc}	Open circuit voltage V
W _s	Wind Speed m/s
X	Concentration Level
η	Proton energy eV
$\eta(\lambda)$	Optical efficiency

- CPV systems are largely based on the use of multi-junction (MJ) solar cells. The electrical output and temperature dependency of these devices are strongly affected by the amount and spectral distribution of the concentrated sunlight [17,18].
- CPV devices use optics to concentrate the light on a small solar cell surface. These devices modify the input spectral distribution and introduce a strong angular dependence on the systems [19,20].
- The cell temperature of CPV systems is difficult to measure and predict. This is due to the fact that the cells mounted on CPV systems are surrounded by several peripheral elements [21,22].
- The direct component of irradiance is the main driver of the electrical output of CPV systems. The direct broadband and spectral distribution of irradiance is more variable and difficult to forecast than the global irradiance, since it is affected more by the presence

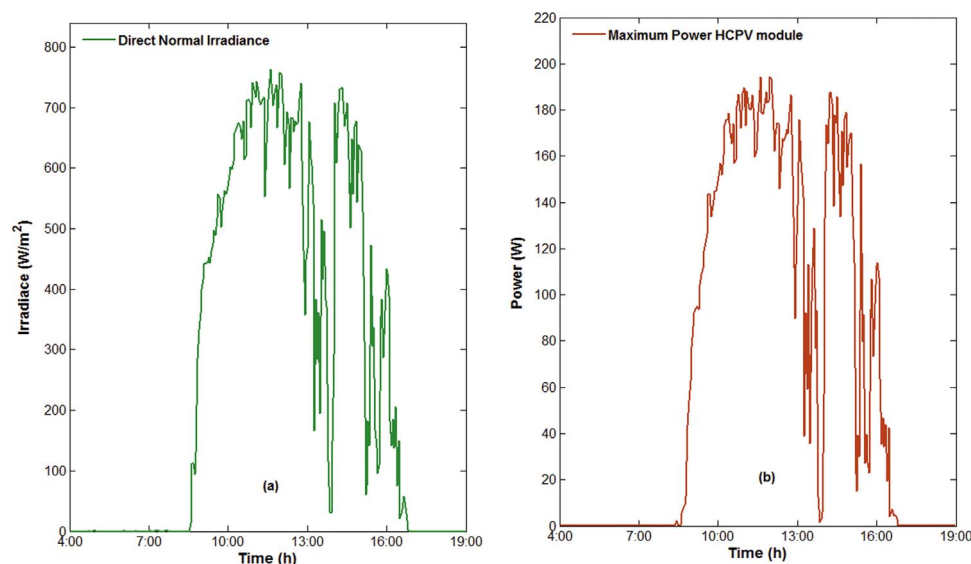


Fig. 1. (a) Direct normal solar irradiance and (b) the maximum power of a typical HCPV module made up of MJ solar cells a Fresnel lenses measure during a summer day at the Centro de Estudios Avanzados en Energía y Medioambiente (University of Jaén).

of clouds and aerosols in the atmosphere [23,24].

In addition to the above, other crucial parameters such as soiling, lens temperature and pointing errors can be reported for playing a relevant role on the performance of CPV systems under real operating conditions [25]. The modelling of CPV systems is consequently complex and challenging from a fundamental point of view.

Artificial Intelligence (AI) techniques, and mainly Artificial Neural Networks (ANNs), have proved to be very helpful in solving complex problems and studying non-linear systems. ANNs have been applied over a wide range of fields for modelling and prediction in energy systems, i.e., for heating, ventilating and air conditioning systems, for modelling and control in power generation systems, for refrigeration [26], and particularly in renewable energy systems, i.e., for modelling of solar steam generators, solar water heating systems or photovoltaic systems [27], among others. In the field of photovoltaics, ANNs have been used to estimate and predict solar radiation data [28–32], the maximum power and normal operating power of a flat photovoltaic module [33,34], to size, model and simulate both standalone and grid-connected PV systems [35,36], to develop photovoltaic systems with a maximum power point tracking controller [37,38], to predict the equivalent circuits parameters of a flat PV module [39], to select a suitable model for characterising PV devices [40], to obtain the I-V curves of different flat plate panels [41,42], or to estimate the energy production of grid connected PV systems [43,44], among others. A complete review of the use of ANNs in photovoltaics can be found in [45].

Due to the advantages offered by the ANNs to solve complex and non-linear problems, and the great level of electrical modelling complexity of CPV devices discussed above, in recent years, several authors have applied various ANNs to solve issues related to LCPV systems and mainly to the HCPV systems. The use of ANNs present the advantage of offering alternative solutions to problems that are still challenging from a fundamental physical point of view, due to the complexity of the different physical phenomena involved in the performance of these systems. Moreover, they also have the advantage that they do not require detailed information about the materials used in the manufacture of the studied system, which are not always available. Additionally, advanced knowledge of semiconductor, optics and/or atmospheric physics and specific software is not required when compared with the most advanced modelling techniques found in the current CPV scientific literature [46,47]. It is also important to note that ANNs also show different disadvantages if compared with tradi-

tional simple analytical and physical solutions. For instance, they require advance knowledge of complex mathematical modelling techniques that are not always easy to manage. In addition, although a high accuracy between the desired input and output variables can be found, the fundamental relationships implicated in the electrical conversion could be sometimes unknown. This may lead to a poor understanding of the CPV device under study.

In this paper, for the first time, a detailed review of the ANNs developed to address various issues related with LCPV and HCPV technologies, is presented. Moreover, a review of the ANN-based models to predict the main atmospheric parameters that affect the performance of CPV system operating in an outdoor environment is also provided. The main features of each specific method are discussed, as well as the different key indicator parameters provided by the different authors.

2. Applications of ANNs to estimate atmospheric parameters

As in any type of PV system the main parameters that influence the output of the CPV devices are solar irradiance, temperature and solar spectrum. In this section a review of ANN-based models for predicting solar irradiance and temperature is conducted since, the use of ANNs to characterise the solar spectrum for CPV applications has not been covered yet.

2.1. Applications of ANNs to estimate the direct and diffuse components of solar radiation

In this section a review of models that are focused on the estimation of the components of solar irradiance, direct or diffuse, is presented. As indicated above, CPV technology is based on the use of optical devices and due to the use of these optical elements, CPV devices react in a different way to the components of solar irradiance.

Thus, for instance, a typical HCPV module is made up of solar cells, optical devices and the rest of the components required to generate electricity and dissipate the heat produced on the solar cell surface. The solar cells used in this technology are based on several p-n junctions, usually three, of type III-V semiconductor alloys. The concentrator optics are based on a primary optical element (usually a point focus Fresnel lens) to collect the sunlight [48] and a secondary optical element that improves the angular acceptance angle of the module and homogenizes the light on the solar cell [49]. Due to the use of point

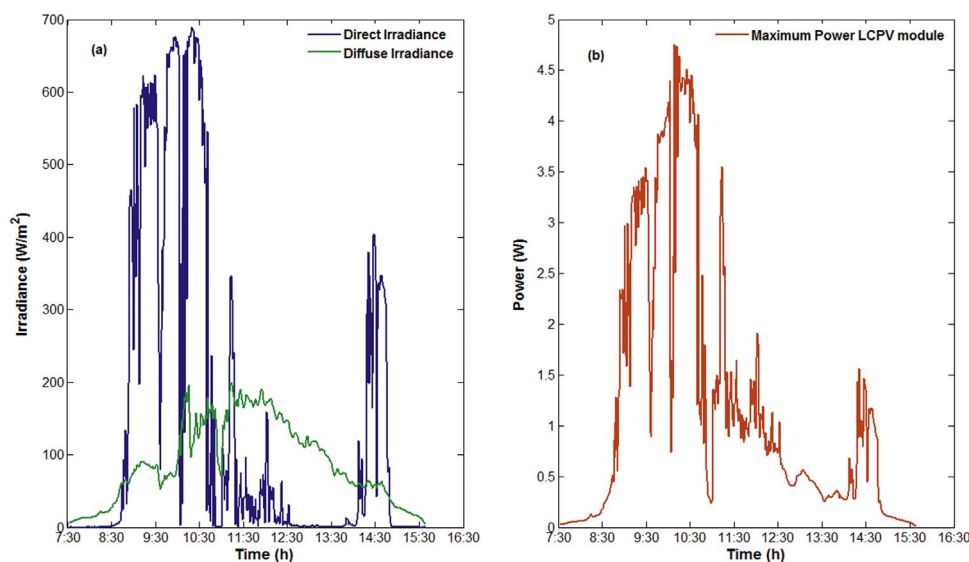


Fig. 2. (a) Direct and diffuse components of irradiance and (b) the maximum power of a LCPV module for this day measured during a winter day at Edinburgh.

Table 1
Summary of ANN-based models for predicting the DNI (or DI) and DHI components of the irradiance.

Authors	Type of ANN	Inputs	Output	Error
Lopez et al.[45]	Bayesian neural network with automatic relevance determination method	<ul style="list-style-type: none"> • K_t • AM 	<ul style="list-style-type: none"> • DNI 	–
Alam et al.[46]	FFNN	<ul style="list-style-type: none"> • Latitude • Longitude • Altitude • Months of year • Mean duration of sunshine per hour • Rainfall ratio • Relative humidity ratio 	<ul style="list-style-type: none"> • RCI 	RMSE (%) = 2.79 to 1.65 MBE (%) = -1.79 to +0.075
Mishra et al. [47]	FFNN RBF	<ul style="list-style-type: none"> • Latitude • Longitude • Altitude • Months of year • Mean Duration of sunshine per hour • Rainfall ratio • Relative humidity ratio 	<ul style="list-style-type: none"> • K_t 	RMSE (%) = 0.8–5.4 RMSE(%) = 7–29
Mellit et al.[48]	FFNN	<ul style="list-style-type: none"> • Hourly Temperature • Humidity • Sunshine duration • Irradiation of hour before 	<ul style="list-style-type: none"> • DNI • DHI 	$R^2(\%) = 98.34$ (DNI) and 98.21 (DHI)
Mubiru et al. [49]	FFNN	<ul style="list-style-type: none"> • Latitude • Longitude • Altitude • Monthly average daily DNI • Sunshine hours • Maximum temperature 	<ul style="list-style-type: none"> • DNI 	$R^2(\%) = 99.8$ $MBE(MJ/m^2) = 0.005$ $RMSE(MJ/m^2) = 0.197$
Marquez and Coimbra[50]	FFNN	<ul style="list-style-type: none"> • Maximum temperature • Temperature • Dew point temperature • Relative humidity • Sky cover • Wind speed • Wind direction • Probability of precipitation • Min temperature • Solar zenith angle • Normalised hour angle 	<ul style="list-style-type: none"> • DNI 	$R^2(\%) = 78.8–82.1$ $MBE(\%) = -8.3$ to -9.5 $RMSE(\%) = 30.1–32.0$
Rodrigo et al.	FFNN	–	<ul style="list-style-type: none"> • DNI 	RMSE = (continued on next page)

Table 1 (continued)

Authors	Type of ANN	Inputs	Output	Error
[51] Rehman and Mohandes[52]	RBF	<ul style="list-style-type: none"> • Day number • Global solar radiation • Ambient temperature • Relative humidity 	<ul style="list-style-type: none"> • DNI • DHI 	MAPE = 0.016 (DNI) and 0.41 (DHI)
Eissa et al.[53]	FFNN	<ul style="list-style-type: none"> • Six SEVIRI thermal channels • Solar zenith angle • Solar time • Day number • Eccentricity correction 	<ul style="list-style-type: none"> • DNI • DHI 	RMSE(%) = 26.1 (DNI) and 25.6 (DHI) MBE(%) = -6.0 (DNI) and +3.6 (DHI)
Chu et al.[54]	FFNN with Genetic algorithm	<ul style="list-style-type: none"> • DNI time-series measured • The cloud coverage time-series 	<ul style="list-style-type: none"> • DNI 	–
Mohammad et al.[55]	FFNN	<ul style="list-style-type: none"> • Six SEVIRI thermal channels • Solar zenith angle • Solar time • Day number • Eccentricity correction 	<ul style="list-style-type: none"> • DNI • DHI 	RMSE(%) = 19.5–34.6 (DNI) and 21.7–26.7 (DHI) MBE(%) = -0.2 to +1.2 (DNI) and -3.1 to +2.6 (DHI)
Renno et al. [56]	FFNN	<ul style="list-style-type: none"> • K_t • Declination angle • Hour angle • Global normal irradiance 	<ul style="list-style-type: none"> • DNI 	MAPE(%) = 5.72 RMSE(%) = 3.15 $R^2=0.992$

focus lenses which concentrate light on the solar cell, the HCPV devices operate only with direct normal irradiance (DNI). So this component of the solar irradiance is essential for the characterization, management and operation of HCPV modules, systems and power plants [50].

In the case of LCPV technology, there are a large number of systems and variations based on very distinct technologies [5]. However, the research trend shows that asymmetric designs of the concentrator are most suitable for LCPV modules for building integration. It has been observed that the performance of stationary low concentration systems largely depends on the sun angle, module temperature and the ability to collect direct (DI) and diffuse (DHI) irradiance. The wide range of acceptance angles of low concentrating devices enables the system to collect both direct and a large portion of diffuse irradiance. However, the amount of collection of diffuse irradiance differs from the direct irradiance, so it needs to be treated differently [51,52].

To illustrate this, Fig. 1 shows an example of how the maximum power of a HCPV module varies with the DNI, while Fig. 2 shows an example the variation of the maximum power of a LCPV module with the DI and DHI components of the irradiance.

It is worth to mention that HCPV technology only uses the DNI due to the use of point focus lenses, and therefore, its low acceptance angle, as previously mentioned. On the other hand, the wider acceptance angle of LCPV systems allows not only the DNI, but also the DI to be collected. It is important to note that the DNI represents the irradiance received on a surface facing directly toward to the sun, so that the solar

rays are always perpendicular to that surface. On the other hand, the DI on a plane of a LCPV system can be simply obtained from the DNI and its incident angle on the surface of the LCPV module as:

$$DI = DNI \cos(\theta) \quad (1)$$

where θ is the incident angle.

Although there are a large number of methods to estimate the global irradiance (GHI), both analytical and artificial intelligence based techniques [53], the DNI is affected by phenomena that are very difficult to forecast. These phenomena, such as cirrus clouds, wildfires, dust storms, and episodic air pollution events, can reduce DNI (or DI) by up to 30% on otherwise cloud-free days [54]. A similar behaviour can be observed with the DHI. Because of this, the modelling and prediction of the DNI (or DI) and DHI is a difficult task and several authors have used ANN-based models to address this issue. These ANNs-based models are briefly described below and Table 1 summarises their main features used to estimate the DNI (or DI) and DHI.

Lopez et al. [55] developed a Bayesian artificial neural network for modelling the DNI. The authors also used a relevance determination method to find the relative relevance of a large set of meteorological and radiometric variables. Results of this method showed that the clearness index (K_t) and air mass (AM) are the more relevant parameters. However, the analysis of the errors was not provided.

In Ref. [56] an ANN model used to indirectly estimate the beam solar radiation from a new parameter, the reference clearness index (RCI), was developed. This parameter is defined as the ratio of the measured beam solar radiation at normal incidence to the beam solar radiation as computed by Hottel's clear day model. The root mean square error (RMSE) of the models varies between 1.65–2.79% for various Indian regions.

Mishra et al. [57] developed self-consistent models for the estimation of direct solar radiation for the Indian climatic zone. Two ANN-based models were used for the indirect estimation of the DNI from the K_t : a feed-forward back-propagation neural network (FFNN) and a radial basis function network (RBF). The results showed the good agreement of the predictions with the measurements for the Indian region, with a RMSE ranging from 0.8% to 5.4% for the FFNN, and 7–29% for the RBF.

In Ref. [58], an adaptive model for predicting the hourly GHI, DHI and DNI was presented. The proposed model was also compared with a FFNN. The results showed that FFNN performed better than the designed adaptive alpha-model, being able to predict the DHI and DNI with acceptable accuracy at Jeddah (KSA), with a correlation coefficient (R^2) of 98.34% for the direct normal irradiance and 98.22%

for the diffuse irradiance.

Mubiru [59] studied different architectures of ANNs in order to develop the most suitable model for estimating of monthly average daily direct solar radiation. The results showed a correlation coefficient of 0.998, a mean bias error (MBE) of 0.005 MJ/m² and the root mean square error of 0.197 MJ/m².

In [60], several forecasting models for hourly solar irradiance (DNI and GHI) using artificial neural networks were developed. The meteorological data used were obtained from the US National Weather Service forecasting database, and solar geotemporal variables were used as inputs. In order to select the more relevant inputs, the gamma test combined with a genetic algorithm was used. According to the authors, it was found that the DNI is much more difficult to predict reliably; RMSE obtained on same-day forecasts are in the range of 28–35%.

Rodrigo et al. [61] developed different architectures of Multilayer Perceptron (MLP) neural network for the generation of DNI hourly time series for a number of Spanish locations. The models were tested in Spanish locations and the results showed that the ANNs perform better for locations placed at the south of Spain. The developed models could be a useful tool for the estimation of the energy that will be produced by concentrating photovoltaic systems, to perform economic analysis and supervise plant operation.

Rehman and Mohandes [62] developed a RBF network to model the DHI and DNI for locations in KSA. The inputs of the model were the day number, global solar radiation, ambient temperature and relative humidity. The results indicate that the proposed model predicts direct normal solar radiation with a mean absolute percentage error (MAPE) of 0.016 and 0.41 for diffuse solar radiation.

Eissa et al. [63] developed a statistical model based on an ensemble artificial neural network (E-ANN) approach for predicting the DHI and the DNI. The inputs of the model were six SEVIRI (on-board Meteosat Second Generation satellite) thermal channels along with several time and seasonal dependent parameters, namely the solar zenith angle, solar time, day number and eccentricity correction. The results were very promising when estimating the solar irradiance at a 15 min temporal resolution and a 3 km spatial resolution. For a totally independent dataset for all sky conditions, RMSE were 26.1% for DNI and 25.6% for DHI, while the MBE were –6% for DNI and +3.6% for DHI.

Chu et al. [64] designed a novel smart forecasting model for intra-hour DNI. ANN optimization schemes in combination with sky image processing were used by authors. The hybrid forecast models achieved statistically robust forecasting skills in excess of 20% over persistence

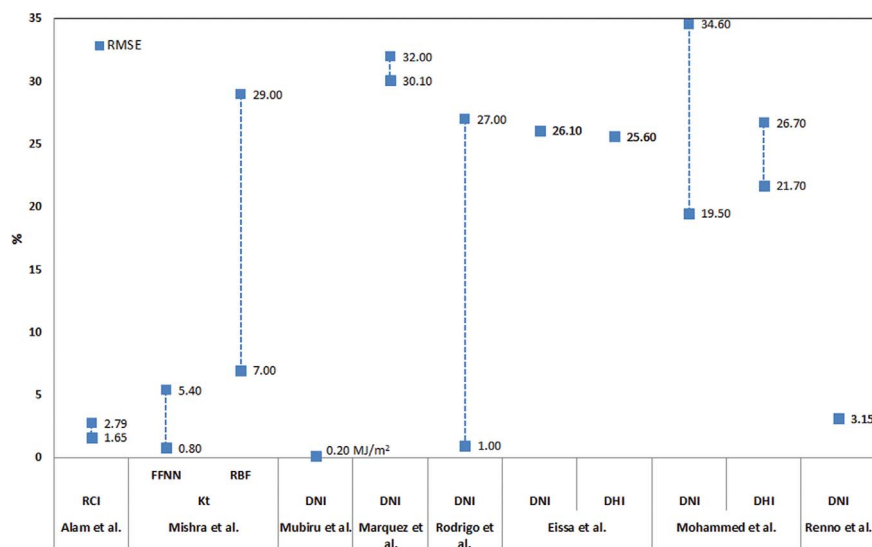


Fig. 3. RMSE of the different method analysed for the estimation of the components of the irradiance DNI (or DI) and DHI.

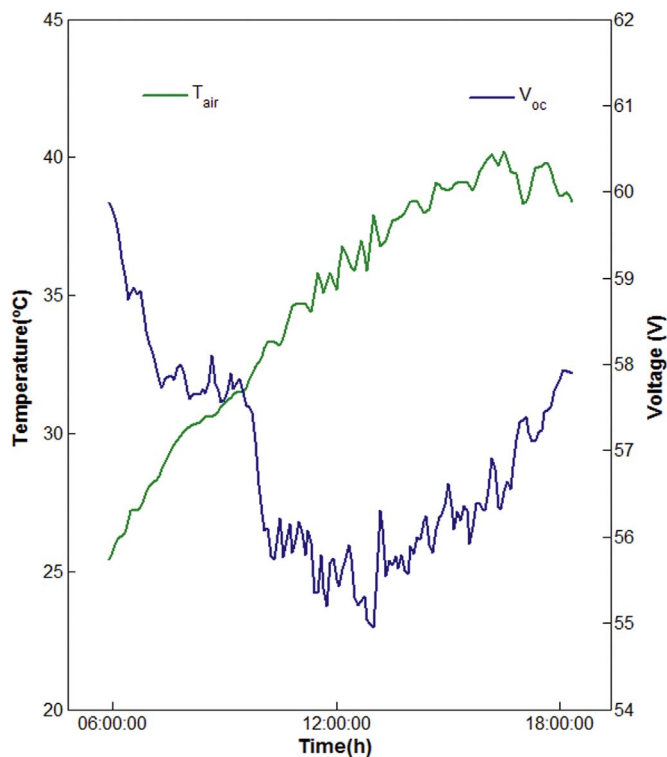


Fig. 4. Ambient temperature and open circuit voltage of a typical HCPV module made up of MJ solar cells a Fresnel lenses measure during a summer day at the Centro de Estudios Avanzados en Energía y Medioambiente in Jaen (University of Jaén).

for both 5 and 10 min ahead forecasts, respectively.

Mohammad et al. [65] proposed an ANN ensemble framework used to estimate the solar irradiance components, DHI, DNI, and GHI. Cloud-free and cloudy observations, for DHI, and DNI, were considered as two separate case studies. In each case study, two E-ANN models were trained; one model for predicting the DHI and the other for predicting the DNI. For the cloud-free case, the RMSE were around 19.5% for DNI and 21.7% for DHI, while MBE were -0.2% for DNI and -3.1% for DHI. For cloudy observations the RMSE were 34.6% for DNI and 26.7% for DHI, while the MBE were $+1.2\%$ for DNI and $+2.6\%$ for DHI.

Recently, Renno et al. [66] have developed a MLP model for predicting the DNI. Different parameters such as climatic, astronomic and radiometric variables have been chosen as inputs, the K_t , declination angle, hour angle, global normal irradiance. The MLP network was trained, tested and validated for the hourly DNI estimation obtaining the MAPE, RMSE and R^2 statistical index values, equal to 5.72%, 3.15% and 0.992 respectively.

As can be seen from Table 1, most of the authors have used feed-forward back-propagation artificial neural networks to predict the components of the irradiance DNI (or DI) and DHI. The majority of the methods are based on atmospheric parameters (temperature, humidity, etc.) and astronomic and radiometric variables (longitude, latitude, solar zenith angle, etc.) as input variables. Regarding the methods that predict the DNI (or DI), the analysis of the errors provided by authors shows that the method proposed by Alam et al. [56] and the method proposed by Mishra et al. [57] based on FFNN present the best results with RMSE values ranging from 2.79 to 1.65% and 0.8 to 5.4%, respectively. However, it is important to highlight that neither of them directly gives the DNI (or DI) as the output parameter. The method proposed by Alam et al. [56] provides as output a new parameter called the reference clearness index (RCI), while the method proposed by Mishra et al. [57] provides K_t as output. Among the methods that directly provide the DNI as output, the method developed by Renno et al. [66] is the one that yields the best results with a RMSE

of 3.15%. With regards to the DHI, it should be noted that only a few methods provide this parameter, and that the RMSE value found is around to be 24% for all cases studied. These results are graphically shown in Fig. 3, where the distribution of the RMSE of the considered methods is represented. It is important to remark that only the methods that provide the RMSE have been taken into account in this analysis. This parameter has been selected since is the most widely used by the different authors to evaluate their methods.

2.2. Applications of ANNs to estimate the ambient temperature

The temperature is another atmospheric parameter that has a significantly influence on the output of PV devices and consequently affects the performance of concentrator photovoltaic devices. To illustrate this, Fig. 4 shows for an example day the evolution of the open circuit voltage (V_{oc}) of a HCPV module with the ambient temperature (T_{air}).

Usually time series of ambient temperature, T_{air} are available in most of the weather stations databases. However, several authors have applied ANN-method to predict this parameter in regions where the availability of data is limited or they do not exist. Furthermore, ANNs have been used for short-term forecast time-series of T_{air} . The ANNs-based models are described below and Table 2 summarises their main features used to estimate T_{air} .

In [67] authors used artificial neural network to predict the hourly mean values of T_{air} twenty-four hours in advance, in Saudi Arabia. The only input to the model is temperature while the output is the temperature of the following day at the same hour. The RMSE is 1.75°C while the mean percent deviation between the predicted and measured values is found to be 3.16, 4.17 and 2.83 for three different years.

Abdel-Aal [68] proposes an abductive network as an alternative machine learning approach to hourly temperature forecasting. The dataset used consists of measured hourly temperature data for Seattle (USA) over a seven years period. The author developed several models to predict the next-day hourly values of temperature and the temperature at the next-hour. The mean absolute errors (MAE) are 2.02°F and 1.05°F respectively, while the MAPE values are 3.19% and 2.14%, respectively.

Smith et al. [69] proposed a ward-style ANN for the prediction of T_{air} during the entire year based on near real-time detailed weather data collected by the Georgia Automated Environmental Monitoring Network (AEMN). Current values and twenty-four hours duration of prior observations for T_{air} , solar radiation, wind speed, rainfall, and relative humidity from the time of prediction were used as inputs for the ANN models. The ANNs were able to provide predictions throughout the year, with a mean absolute error (MAE) of the year-round models that was less during the winter months than the MAE of the models resulting from the application of previously developed winter-specific models. The prediction MAE for a year-round evaluation set ranged from 0.516°C at the one-hour horizon to 1.873°C at the twelve-hour horizon.

Dombaycı and Gölcü [70] proposed an ANN to predict daily mean T_{air} in Denizli, Turkey. The ANN was trained with temperature values measured by the Turkish State Meteorological Service over a three years' period (2003–2005). The temperature values for the year 2006 were used as testing data. The inputs of the network were the month, day and the mean temperature value of the previous day. Several ANNs was trained and the best results were obtained for the network having 6 hidden neurons. The R^2 and the RMSE values of this network were 0.99 and 1.85 for the training dataset. As for the testing dataset, these values were 0.98 and 1.96, respectively.

Deligiorgi et al. [71] proposed several ANNs for temporal and spatial estimation of the air temperature. For the temporal forecasting of air temperature, separate ANNs were trained for predicting the T_{air} one hour, two hours and three hours ahead using the Levenberg-

Table 2
Summary of ANN-based models for predicting T_{air} .

Authors	Type of ANN	Inputs	Output	Error
Tasadduq et al.[57]	FFNN	<ul style="list-style-type: none"> Hourly T_{air} 	<ul style="list-style-type: none"> Next-day hourly T_{air} 	Mean percent deviation=2.83–4.17 RMSE=1.75
Abdel-Aal[58]	Abductive network	<ul style="list-style-type: none"> 24 hourly temperatures for day Extreme temperatures for day Forecasted extreme temperatures for next day 	<ul style="list-style-type: none"> Next-day hourly T_{air} 	MAE (°F)=1.68 MAPE (%)=3.19
	Abductive network	<ul style="list-style-type: none"> 24 hourly temperatures for day Available hourly temperatures on day Extreme temperatures for day Forecasted extreme temperatures for next day 	<ul style="list-style-type: none"> Next-hour T_{air} 	MAE(°F)=1.05 MAPE (%)=2.14
Smith et al.[59]	Ward-style ANN	<ul style="list-style-type: none"> Air temperature Solar radiation Wind speed Rainfall Relative humidity 	<ul style="list-style-type: none"> T_{air} at different hour horizon (1–12 h) 	MAE (°C)=0.52 (1 h) to 1.87 (12 h)
Dombaycı and Gölcü[60]	FFNN	<ul style="list-style-type: none"> Monthly T_{air} Daily T_{air} The mean temperature value of the previous day 	<ul style="list-style-type: none"> Mean daily T_{air} 	R^2 =0.99 (training set) and 0.98 (test set) RMSE=1.85 (training set) and 1.96 (test set)
Deligiorgi et al.[61]	FNFN	<ul style="list-style-type: none"> The current and the five previous T_{air} observations 	<ul style="list-style-type: none"> T_{air} at different hour horizon (1 h, 2 h and 3 h) 	R =0.99 (1 h), 0.97 (2 h) and 0.94 (3 h) R^2 =0.98 (1 h), 0.94 (2 h) and 0.89 (3 h) MBE (°C)=−0.07 (1 h), −0.23 (2 h) and −0.41 (3 h) MAE (°C)=0.59 (1 h), 1.00 (2 h) and 1.36 (3 h) RMSE(°C)=0.84 (1 h), 1.43(2 h) and 1.90 (3 h) d =0.99 (MLP) and 0.99 (RBF)
	MLP RBF	<ul style="list-style-type: none"> Mean hourly T_{air} data from six meteorological stations 	<ul style="list-style-type: none"> Spatial estimation of T_{air} 	R =0.98(MLP) and 0.98 (RBF) R^2 =0.96 (MLP) and 0.96 (RBF) MBE (°C)=−0.01 (MLP) and 0.03 (RBF) MAE (°C)=0.82 (MLP) and 0.87 (RBF) RMSE(°C)=1.07 (MLP) and 1.12 (RBF) d =0.99 (MLP) and 0.99 (RBF)
Almonacid et at[62]	MLP	<ul style="list-style-type: none"> Daily maximum T_{air} Daily minimum T_{air} Daily mean T_{air} Latitude Altitude 	<ul style="list-style-type: none"> Hourly T_{air} 	RMSE (°C)=0.53–1.28 RMSE (%)=2.81–8.08
Cobaner et al.[63]	FFNN	<ul style="list-style-type: none"> Latitude Longitude Altitude Month number 	<ul style="list-style-type: none"> Maximum T_{air} Minimum T_{air} Average T_{air} 	MAE (%)=2.99 (max), 4.28 (min) and 3.08 (average) MSE (%)=14.75 (max), 30.04 (min) and 16.35 (average) R^2 =0.778 (max), 0.772 (min) and 0.780 (average)
	ANFI			MAE (%)=1.74 (max), 2.83 (min) and 1.25(average) MSE (%)=5.06(max), 14.48 (min) and 2.58 (average) R^2 =0.925 (max. temp), 0.890 (min) and 0.966 (average)
Kisi and Shirir[64]	FFNN	<ul style="list-style-type: none"> Month number 	<ul style="list-style-type: none"> Long-term monthly T_{air} 	R^2 =0.99 to 0.92
	ANFI	<ul style="list-style-type: none"> Latitude Longitude Altitude 		R^2 =0.99 to 0.88

Marquardt back propagation algorithm. It was found that the ANNs performance was decreased with increasing the forecasting lag. In all cases the MAE was less than 1.4 °C and the variance decreased from 97.7% for the one hour ahead to 88.7% for the three hours ahead. For the spatial estimation the RBF and MLP predictions non-linear FFNN schemes were compared. From the analysis of the results authors concluded that both models gave accurate air temperature, estimated

with MAE values less than 0.9 °C, with very high index of agreement (d) values and minimal biases. Furthermore, the variance was 95.9% for the RBF model and 96.3% for the MLP scheme.

Almonacid et al. [72] proposed an ANN-based model for estimating the hourly series of T_{air} in Spain. The inputs of the model were the daily maximum, minimum and the daily mean air temperatures, latitude and altitude. The results were compared with the ones estimated by

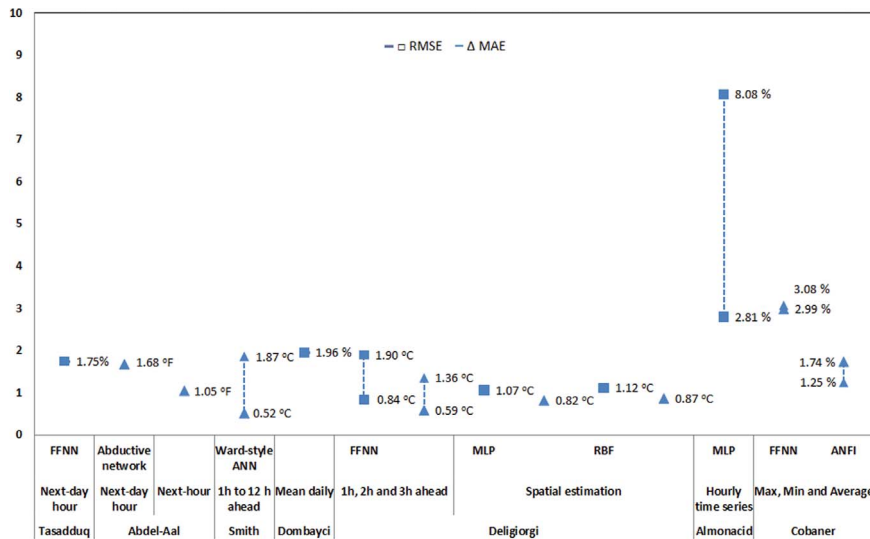


Fig. 5. RMSE and MAE values of the methods for estimating the air temperature provide by the authors.

Table 3
Summary of ANN-based models for modelling MJ solar cells.

Authors	Type of ANN	Inputs	Output	Error
Patra and Patra et al. [73,74]	MLP	<ul style="list-style-type: none"> λ Voltage 	<ul style="list-style-type: none"> Tunnelling effects of a DJ solar cell EQE of a DJ solar cell Current density at one sun of a DJ solar cell Current density in dark of a DJ solar cell 	$R^2 = 0.99$ (TJ) and 0.99 (EQE)MSE = 30.63 (TJ) and -29.67 (EQE) $R^2 = 0.99$ (1sun) and 0.99 (dark) MSE = -20.02 (1sun) and -58.90 (dark)
Patra[76]	Chebyshev Neural Network	<ul style="list-style-type: none"> λ Voltage 	<ul style="list-style-type: none"> Tunnelling effects of a DJ solar cell EQE of a DJ solar cell. Current density at one sun of a DJ solar cell. Current density in dark of a DJ solar cell. 	$R^2 = 0.99$ (TJ) and 0.99 (EQE)MSE = 31.50 (TJ) and -31.17 (EQE) $R^2 = 0.99$ (1sun) and 0.99 (dark) MSE = -14.30 (1sun) and -52.10 (dark)
Patra and Maskell[77]	MLP	<ul style="list-style-type: none"> λ η f 	<ul style="list-style-type: none"> EQE of a TJ solar cell 	$R^2 = 0.99$ (top), 0.99 (middle) and 0.99 (bottom) MSE(db) = 2.11(top), 2.34(middle) and 6.55(bottom)
Fernández et al.[78]	FFNN	<ul style="list-style-type: none"> X SMR T_c 	<ul style="list-style-type: none"> I_{sc} a TJ solar cell V_{oc} a TJ solar cell P_{max} a TJ solar cell 	RMSE(%) = 0.00 (I _{sc}), 0.12 (V _{oc}) and 0.48 (P _{max}) MBE(%) = 0.00 (I _{sc}), 0.01 (V _{oc}) and -0.08 (P _{max})

classical methods. Absolute RMSE values ranging from 0.53 to 1.98 °C and relative RMSE values from 2.81% to 8.08% were obtained.

Cobaner et al. [73] proposed the use of artificial neural networks (ANN), adaptive neuro-fuzzy inference system (ANFIS), and multiple

linear regression (MLR) models to estimate the means of maximum, minimum, and average monthly temperatures as a function of geographical coordinates and month number for any location in Turkey. The latitude, longitude, and altitude of the location, and the month number are used as the input variables, and each of the mean monthly maximum, minimum, and average air temperatures is computed as the output variable. The ANFIS-based model provided the best result with a MAE ranging from 1.25% for the average temperature to 2.83% for the minimum temperature, mean square error (MSE) ranging from 2.58% for the average temperature to 14.48% for the minimum temperature and R^2 ranging from 0.890 for the minimum temperature to 0.966 for the average temperature.

Kisi and Shiri [74] proposed the use of ANFIS and ANN models for predicting the long-term monthly T_{air} values at 30 weather stations of Iran. Monthly data of 20 weather stations were used for training. The number of the months, station latitude, longitude and altitude values were used as input parameters. The ANN model generally performed better than the ANFIS model in the test period. For the ANN model, the maximum and minimum correlation coefficient values were found to be 0.99 and 0.92 in Semnan and Bandar-e-Abbas.

As can be concluded from the summary of ANN models presented in Table 2, in contradiction to the case of predicting the different components of irradiance, several types of ANNs have been used to forecast the air temperature. The majority of the methods use atmospheric parameters and some radiometric variables as inputs. Regarding the output, the proposed methods provide the T_{air} at different time-scales, such as T_{air} at different hourly horizons (1 h, 2 h, etc.), next-day hourly T_{air} , maximum, minimum and average values of T_{air} , and time-hourly series of T_{air} . The authors also provide different statistical parameters to evaluate the models proposed, so an easy comparison among them is unfortunately not direct in most of the cases. Despite of this, from the analysis of the errors, it can be concluded that ANNs are an accurate tool to predict the T_{air} , with RMSE values less than 3% (or 2 °C), MAE values less than 3% (or 3 °C), MAPE values around 3% and R^2 values of 0.9 for most of the cases. As a summary, Fig. 5 graphically shows the most widely used statistical parameters to evaluate the proposed methods by the different authors, namely RMSE and MAE.

3. Application of ANNs to the electrical modelling of CPV devices

As in any kind of energy system, modelling the electrical output of a photovoltaic device is crucial for the system design and its energy

Table 4
Summary of the main features of ANN-based models for modelling CPV devices.

Authors	Type of ANN	Inputs	Output	Error
Fernández et al.[65]	FFNN	<ul style="list-style-type: none"> ● DI ● DHI ● T_m ● Transverse angle ● Longitudinal angle 	<ul style="list-style-type: none"> ● P_{max} of a LCPV module 	$R^2 = 0.99$ RMSE (%) = 2.32 MBE (%) = -0.05
Fernandez and Almonacid[79]	FFNN	<ul style="list-style-type: none"> ● AM ● AOD ● PW 	<ul style="list-style-type: none"> ● DNI_c 	$R^2 = 0.98$ RMSE (%) = 2.92 MBE (%) = 0.07
Fernández et al.[69]	FFNN	<ul style="list-style-type: none"> ● DNI ● T_{air} ● W_s 	<ul style="list-style-type: none"> ● T_c of a HCPV module 	$R^2 = 0.95$ RMSE (%) = 4.80 RMSE ($^{\circ}C$) = 3.24
Fernández and Almonacid[80]	FFNN	<ul style="list-style-type: none"> ● DNI_{heat} ● T_{air} ● W_s 	<ul style="list-style-type: none"> ● T_{h-k} of a HCPV module 	NRMSE (%) = 2.93 ARMSE ($^{\circ}C$) = 1.76 MAE ($^{\circ}C$) = 1.13 MBE (%) = -0.04 MRE (%) = -0.15
Almonacid et al.[84]	FFNN	<ul style="list-style-type: none"> ● DNI ● AM ● PW ● T_{air} ● W_s 	<ul style="list-style-type: none"> ● P_{max} of a HCPV module 	$R^2 = 0.99$ RMSE (%) = 2.91 MBE (%) = 0.12
Rivera et al. [85]	RBF with a cooperative-competitive hybrid algorithm	<ul style="list-style-type: none"> ● DNI ● APE ● T_{air} ● W_s 	<ul style="list-style-type: none"> ● P_{max} of a HCPV module 	RMSE (%) = 3.3
Almonacid et al.[88]	FFNN	<ul style="list-style-type: none"> ● DNI_c ● T_c 	<ul style="list-style-type: none"> ● I-V characteristic of a HCPV module 	RMSE (%) = 0.19–1.66 MBE(%) = 0.38–0.40
García-Dominguez et al.[89]	FFNN	<ul style="list-style-type: none"> ● DNI ● APE ● T_{air} ● W_s 	<ul style="list-style-type: none"> ● I-V characteristic of a HCPV module 	AE(%) = 3.73 (MLP _{vt}) and 3.72 (MLP _{pa})

prediction. However, as it is indicated previously, the electrical modelling of CPV modules and systems shows a significantly greater level of complexity than conventional PV technology. Moreover, this level of complexity is increased in HCPV technology due to the use of MJ solar cells. Because of this difficulty, in recent years the scientific community has devoted efforts in developing ANN-based models which try to solve some of these issues. These models are mainly focused on the prediction of the maximum power or the I-V characteristic of this kind of devices, but also on the modelling of the behaviour of MJ solar

cells, on the estimation of the cell temperature (T_c) or the spectral dependence of these devices. In the next subsections, the ANNs based models developed to address some of the issues related with the CPV technology, are presented. Tables 3 and 4 summarise the main features of these ANN-models used in the field of the CPV technology.

3.1. Applications of ANNs to LCPV technology

One of the problems of LCPV technology is the lack of models to calculate directly the maximum power. This is mainly due to the fact that the performance of these systems largely depends on the sun angle, module temperature and the ability to collect the DHI and the DI. However, as previously mentioned, the amount of collection of DHI differs from the DI, so it needs to be treated differently [51].

To address this issue Fernández et al. developed an ANN-based model to estimate the maximum power of a LCPV module [75]. The model takes into account all the main important parameters that influence the electrical output of these kinds of systems such as the direct irradiance, diffuse irradiance, module temperature and the transverse and longitudinal incidence angles. Fig. 6 shows the actual and the estimated maximum power using the ANN-based model proposed for two example days summer (left) and winter (right), i.e., high and low irradiance levels. The R^2 , the RMSE and the MBE values of this network were 0.99 and 2.32% and -0.05%, respectively.

It should be noted that a few models for the electrical characterization of low concentrator photovoltaic modules have been reported [76] and that there are no models in literature that allow the direct calculation of the maximum power of a LCPV module under real conditions and which take into account all the parameters that influence its electrical performance, such as the direct irradiance, diffuse irradiance, module temperature and the transverse and longitudinal incidence angles. Currently, the ANN based-model is the only one that has taken into account all parameters that affect the output of a LCPV device, being able to predict the maximum power of a LCPV module with a great level of accuracy for any operating condition. This model allows the behaviour of a module with the same characteristics to be analysed in a wide range of operating conditions, being a useful tool for designers and researchers. Furthermore, the ANN-based model could be adapted to a large number of systems and variations based on very distinct technologies [5] of the LCPV technology, as it is a useful tool for designing and evaluating the performance and profitability of LCPV technology.

3.2. Applications of ANNs to HCPV technology

In the field of HCPVs, due to their complexity, the ANNs have been used to solve different issues related with this new technology. For instance, this technology is based on the use of high-efficiency solar cells made of several p-n junctions of compound semiconductors whose electrical behaviour is more complex to model than single-junction solar cells. Furthermore, due to the use of multi-junction solar cells and concentrator optics, HCPV modules and systems show a strong dependence on the solar spectrum. The way to quantify the spectral changes and evaluate how these affect the output of a HCPV device is not a trivial issue [19,77]. In addition, as in conventional PV technology, the cell temperature is an important input in models used for the electrical characterization of HCPV devices since the high temperature at which the cells of a HCPV module are working due to solar concentration affects its performance. However, one of the problems in HCPV technology is that the direct measurement of this temperature is complex because it requires access inside the module [21,22,78].

A complete review of the ANN applications in the HCPV field is presented in this section.

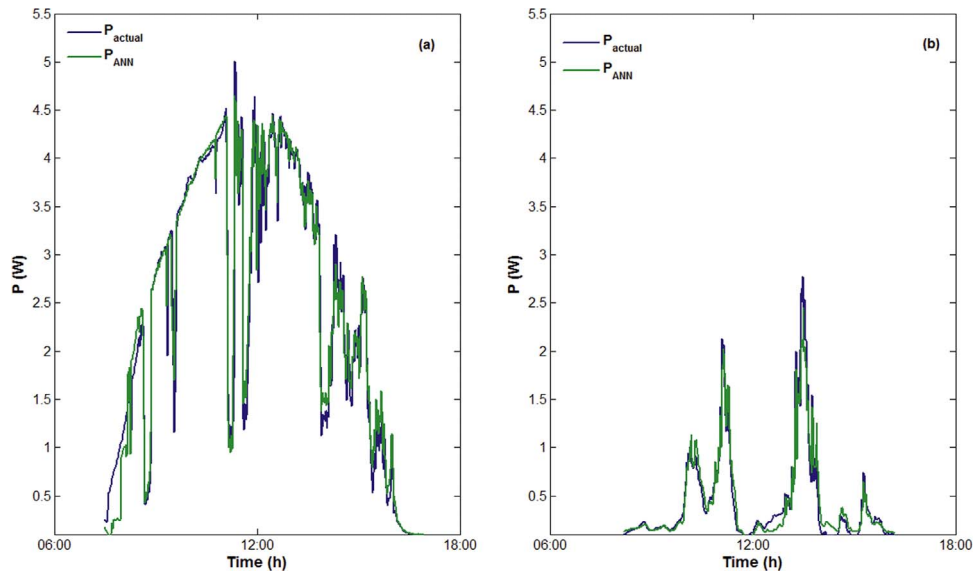


Fig. 6. Example of actual and estimated maximum power using the ANN-based model proposed in [75] for two example days: (a) summer and (b) winter.

3.2.1. Applications of ANNs to model multi-junction solar cells

While LCPV and MCPV systems are based on single-junction solar cells, usually Si-crystalline, the solar cells used in HCPV technology, are made of several p-n junctions of III-V semiconductor alloys of the Periodic Table. The aim of these cells is to optimize the absorption of the solar spectrum and increase the efficiency of the solar cell electricity conversion [79]. However, the internal series connection of several junctions with different band gap energies makes these devices extremely sensible to the incident spectrum. Thus, while single-junction solar cells are mainly influenced by changes in irradiance and temperature, multi-junction solar cells show complex behaviour as their performance is also strongly influenced by changes in the solar spectrum. Due to this, several approaches based on artificial neural network have been proposed in order to characterize these devices.

In [80,81] Patra et al. developed four MLPs to characterize dual-junction (DJ) GaInP/GaAs solar cells; one for estimating the tunnelling

effects of a DJ solar cell, and the other three for estimating the External Quantum Efficiency (EQE) and the I-V characteristic, both under 1 sun and in dark. The ANNs use as input the voltage for estimating the tunnelling effects, and the I-V characteristic and the irradiation wavelength (λ) for estimating the EQE. The results showed that the predicted parameters with the ANNs developed are more closely to the experimental ones than the simulated data obtained through the Silvaco ATLAS software [82].

Following the same approach as in the previous case in [83] a novel Chebyshev neural network-based model to predict the EQE and the I-V characteristics (both at one sun and dark levels) for a DJ GaInP/GaAs solar cell, was presented.

Patra and Maskell [84] also developed an ANN-based model to estimate the EQE and the performance of triple-junction (TJ) InGaP/GaAs/Ge solar cells under the influence of a wide range of charged particles. The model use the wavelength (λ), the proton energy (η) and

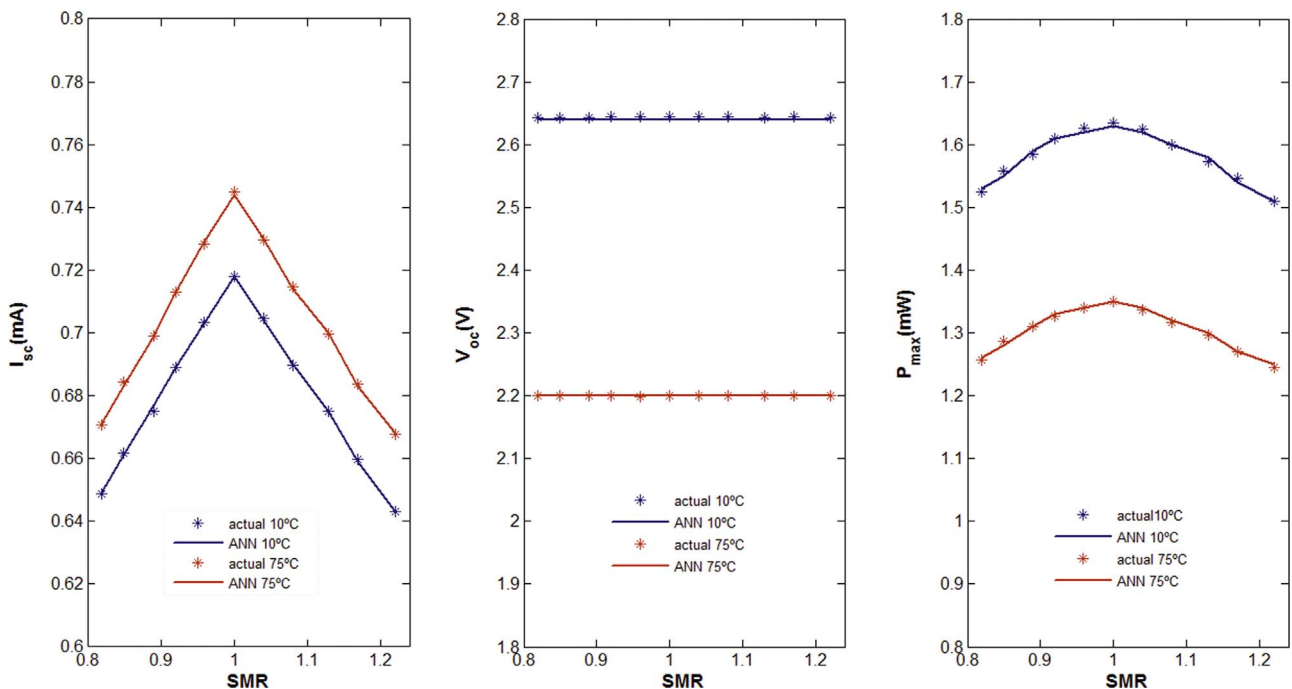


Fig. 7. Example of the actual and predicted electrical parameters of a TJ solar cells using the ANN-based model presented in [85] versus SMR for two different temperatures (X=1).

fluence (f) as inputs. From the analysis of the results presented by the authors it can be concluded that the ANN models developed perform quite well for the estimation of EQE of the solar cell under the influence of proton energy ranging from 30 keV to 10 MeV with fluence levels ranging from 10^{10} to 10^{14} ion/cm².

Fernández et al. [85] proposed three ANN based-models for modelling the main electrical parameters of a TJ solar cell, i.e., short-circuit current (I_{sc}), open circuit voltage (V_{oc}) and maximum power (P_{max}). The inputs of the ANNs were the concentration level (X), spectral matching ratio (SMR) and cell temperature (T_c). Fig. 7 shows some examples of the actual and predicted electrical parameters using the ANN-based model versus SMR. Results show that the models accurately estimate the main electrical parameters of a TJ solar cell with a RMSE lower than 0.5% and a MBE almost 0%.

It is important to note that modelling the electrical behaviour of MJ solar cells is a crucial task for designing and evaluating the performance and profitability of HCPV technology. The main problem is that these devices show a complex behaviour under concentrated sunlight, spectrum and cell temperature, and the ability to obtain the electrical parameters of MJ solar cells at any desired working condition remains challenging since the previous models that address this issue, estimate the parameters at a particular set of operating conditions. The ANN-based models developed, offer an excellent and alternative tool for the simulation of MJ devices when analytical relationships are not available. Furthermore, these ANN-based models could be easily adapted to the new devices that are coming soon such as MJ solar cells based in four junctions or metamorphic solar cells.

Table 3 summarises the main features ANNs-based models for modelling MJ solar cells.

3.2.2. Applications of ANNs to quantify the effective irradiance of a HCPV module

As already indicated, HCPV modules and systems show a strong dependence with the spectrum, due to the use of high-efficiency solar cells made of several p-n junctions of compound semiconductors and concentrator optics. One approach to quantify this spectral dependence is based on the premise that the spectral effects of a HCPV device can be quantified from the effective irradiance (DNI_c) that can be defined as the portion of the incident spectrum that an HCPV device is able to convert into electricity:

$$DNI_c = \frac{\min(\int E_b(\lambda)\eta(\lambda)SR_i(\lambda)d\lambda)}{\min(\int E_{b,ref}(\lambda)\eta(\lambda)SR_i(\lambda)d\lambda)} \int E_{b,ref}(\lambda)d\lambda \quad (2)$$

where the index i represents the junction considered, λ is the wavelength, $SR_i(\lambda)$ is the spectral response of the i -junction, $E_b(\lambda)$ is the spectral distribution of the direct normal irradiance and $\eta(\lambda)$ is the optical efficiency of the HCPV module.

Following this approach, Fernandez et al. presented an ANN-based model to predict the effective irradiance [86]. The inputs used were those atmospheric parameters that have a major influence on the spectral distribution of the direct normal irradiance and so on, in the performance of a HCPV device, namely, the air mass (AM), aerosol optical depth (AOD) and precipitable water (PW). Results show that the ANN-based model is able to predict the effective irradiance with a RMSE of 2.92%, a MBE of -0.12% and a R^2 of 0.98.

3.2.3. Applications of ANNs to quantify the cell temperature of a HCPV module

As in conventional PV technology, the cell temperature is an important input in models used for the electrical characterization of HCPV devices since the temperature at which the cells of a HCPV module are working affects its performance. However, the measurement of this temperature in a HCPV module is a complex task due to its special features that do not allow the cell to be accessed in the majority of the cases without damaging the modules.

To solve this problem an ANN-based model was presented in [78]. This model attempts to characterise the relationship between the cell temperature and the main meteorological parameters that affect its performance. The input parameters are the direct normal irradiance (DNI), air temperature (T_{air}) and wind speed (W_s). Results show that the ANN based-model significantly improves the results of the method based on a lineal expression, with an $R^2=0.95$, a relative RMSE=4.80% and an absolute RMSE=3.24 °C.

Following the approach presented in [78], Fernández and Almonacid, developed an ANN-based model to indirectly predict the cell temperature of a HCPV module connected to an inverter [87]. The aim of this model was to avoid the direct measurement of the cell temperature and so to damage the module, but also take into account that the T_c of a HCPV module connected to an inverter is lower than operating open-circuit voltage since an important part of the light power density is converted into electricity. The inputs of the model were the T_{air} , W_s and the portion of the direct normal irradiance

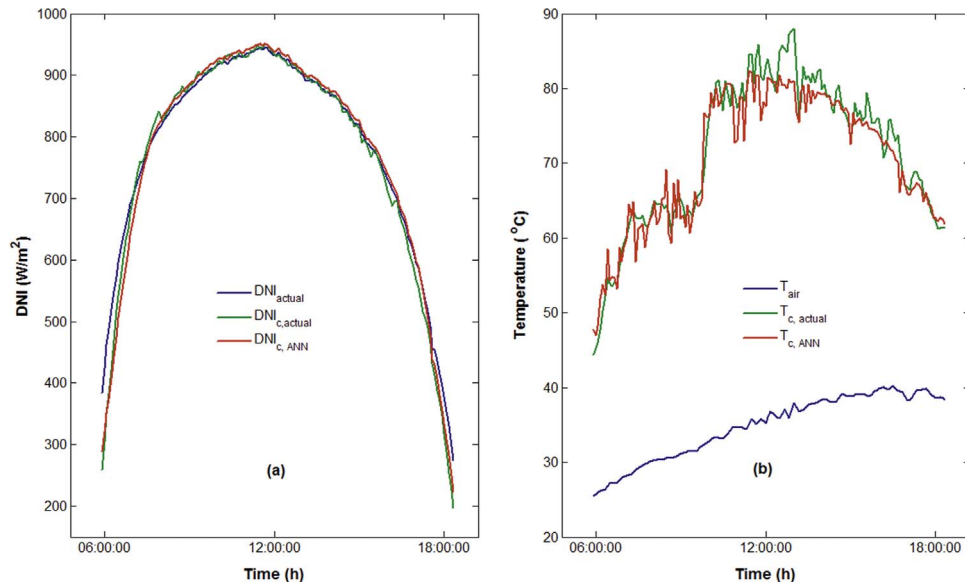


Fig. 8. (a): example of actual DNI_c versus DNI_c predicted by ANN based model presented in [86] for a day (b): example of the T_c of the HCPV module measured during a day versus T_c predicted by the ANN based-model presented in [78].

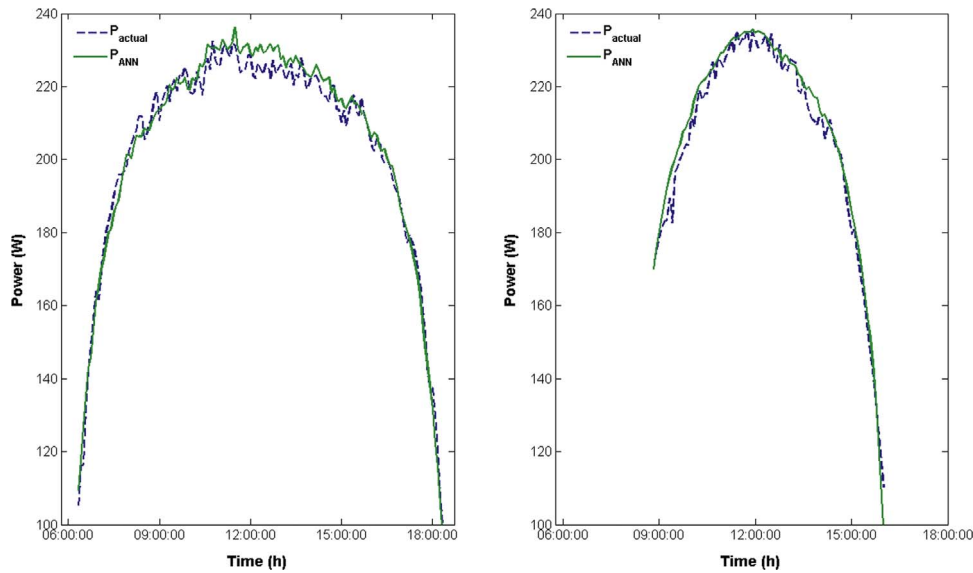


Fig. 9. Example of actual P_{\max} versus predicted maximum power by ANN based model presented in [91] for two day: summer (left) and winter (right).

transformed into heat (DNI_{heat}). The output was the heat-sink temperature (T_{h-s}) of the HCPV module connected to the micro-inverter. Results show that the method predicts the T_c of a module connected to an inverter with a low margin of error with a normalised root mean square error (NRMSE) equal to 2.93%, an absolute root mean square error (ARMSE) equal to 1.76 °C, a MAE equal to 1.13 °C, and a MBE and a mean relative error (MRE) almost equal to 0%.

As mentioned above, the direct measurement of the T_c in HCPV modules requires access inside the module and placing a sensor close to the solar cell on the solar receiver and this is not usually possible without damaging the HCPV module or the elements of the assembly that surround the MJ solar cells. It is worth mentioned that the ANN-based model developed in [87] allows the indirect measurement of this temperature to be done with a great level of accuracy, avoiding the damage of the module. Furthermore, this model is an excellent tool offered to scientific community to calculate this temperature in any CPV device and in any location on the cell since is based only on atmospheric parameters.

As an example of the methods described above, Fig. 8(a) shows the DNI measured during a summer day and the DNI_c measured for this day versus the DNI_c predicted by the ANN based-model presented in [86]. As can be seen from this figure, at the sunrise and sunset the DNI_c measured is lower than the DNI due to higher spectral losses; this

behaviour is also shown by the DNI_c predicted by the ANN. Fig. 8(b) shows an example of the T_{air} for a summer day and the T_c of the HCPV module measured for this day versus the T_c predicted by the ANN based-model presented in [78].

It is important to highlight that a different approach for the electrical modelling of a HCPV device is based on the premise that the electrical parameters of a HCPV module can be estimated by applying models and equations used for conventional PV technology from the direct normal irradiance, corrected spectrally, and the cell temperature [88,89]. Thus, the ANN-based models developed for estimating the spectrally corrected direct normal irradiance and cell temperature could allow the calculation of the electrical parameters of the HCPV devices to be carried out by applying the conventional model used in PV [90]. This will facilitate the study and analysis of these systems to be able to apply simple models widely used by the scientific community.

3.2.4. Application of ANNs to model a HCPV module

As any kind of energy system the electrical characterization of HCPV devices is crucial. It is for this reason that the majority of the ANN-based models developed for HCPV technology are focused to address this issue, i.e., the prediction of the maximum power and the I-V characteristic of this kind of devices.

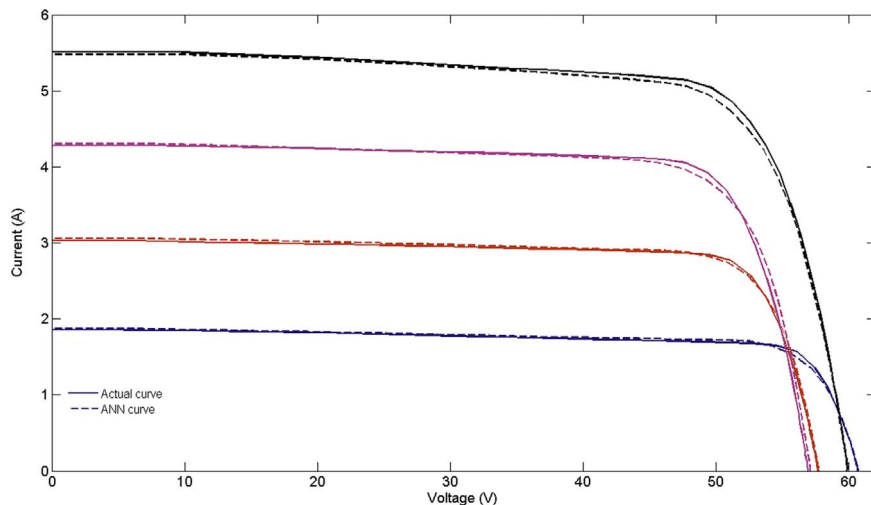


Fig. 10. Example of actual and predicted IV curves using this ANN-based model presented in [95] for different operating conditions.

3.2.5. Application of ANNs to estimate the maximum power of a HCPV module

The output of HCPV modules could be expressed as a function of irradiance (B), spectrum (S), temperature (T) and wind speed (W_s):

$$P_{max} = f(B, S, T, W_s) \quad (3)$$

In order to fit this function, different approaches based on artificial neural network-based models have been proposed, since the relation between these parameters and the electrical behaviour of a HCPV module is complex and nonlinear.

Almonacid et al. [91] developed an ANN-based model to find the relation between the output of a HCPV and the main parameters that affect its performance. The input parameters used by the model are the direct normal irradiance, the air mass and precipitable water to evaluate the spectrum; and the air temperature and the wind speed to evaluate the cell temperature. The results show that the ANN based-model could be used to estimate successfully the output of a HCPV module with a MBE of 0.07%, a RMSE of 2.91% and R^2 of 0.99.

Fig. 9 shows an example of the estimation of the P_{max} of the HCPV module using the ANN based-model presented in [91] for two different days (summer and winter).

Rivera et al. [92] implemented a cooperative-competitive hybrid algorithm for radial basis function networks to estimate the output of a HCPV module. The inputs of the model are the direct normal irradiance, the Average Photon Energy (APE) [93,94], to quantify the spectral influences on the maximum power of a HCPV module, the air temperature and the wind speed. The model obtained gives an absolute error (AE) of approximately 3.3%.

3.2.6. Application of ANNs to estimate the IV characteristic of a HCPV module

The simulation of the complete I-V curve of a PV device is a key factor for the electrical characterization and design of systems and power plants; this issue is especially complex in HCPV due to its inherent features. Thus, several authors have proposed the use of ANNs to address this issue.

Almonacid et al. [95] introduced a method based on ANN and atmospheric parameters for obtaining the I-V curve of a HCPV module as a function of the spectrally corrected direct normal irradiance and cell temperature. The analysis of the results shows that the method accurately predicts the I-V curve of a HCPV module with RMSE values ranging from 0.19 to 1.66% and MBE values ranging from 0.38 to 0.40% for a wide range of operating conditions. Fig. 10 shows some examples of actual and predicted IV curves using this ANN-based

model for different operating conditions.

García-Domínguez et al. [96] proposed two multilayer perceptron (MLP) models which were used to obtain the I-V curve of a HCPV module using as inputs the direct normal irradiance, the air temperature, the wind speed and the average photon energy. The first model consisted of a MLP trained with Cartesian coordinates (MLP_{VI}) and the second model consisted of a MLP trained with polar coordinates (MLP_{PC}). The MLP trained with Cartesian coordinates has an average relative curve area error equal to 3.73%. In the case of the MLP trained with polar coordinates, this model produces an average relative curve area error of 3.72%.

The estimation of the IV curve of a HCPV generator under the time-varying atmospheric parameters is crucial for energy yield assessments and for the design of the electrical requirements and/or protections of a system or power plant. This is also important since the generator works in different regions of its IV curve depending on the regulation and control devices used in each installation and therefore, the complete IV curve needs to be known in order to accurately predict its electrical performance. However, due to its complexity, the estimation of the IV curve of a HCPV module and its validation with long-term measurements outdoors has not been addressed yet with analytical models. Thus, the ANN-based methods allow the IV curve of a HCPV generator to be simulated under the time-varying atmospheric parameters with a low margin of error. Furthermore, the method presented in [95] is also fully based on atmospheric parameter and outdoor measurements so has the advantage that the electrical parameters of a HCPV module can be estimated without detailed information about the materials and characteristics of the module. The use of atmospheric parameters also allows the simulation of the complete IV curve at a desired site provided that the atmospheric parameters are available.

The main features of the different ANNs-based models for modelling CPV devices outlined above can be found in Table 4.

From the methods analysed in this section, it can be concluded that the use of ANNs, mainly feed-forward back-propagation artificial neural networks, provides a very useful and accurate tool to model the electrical behaviour of CPV technology. This offers a valuable approach to carry out an adequate assessment of this new technology and promote its market expansion. At the same time, they provide a precise and alternative rapid solution to solve problems that are still under study by the CPV community from a fundamental physical point of view. This is the case, for instance, of the method introduced in [85] to predict the I-V dynamics of MJ solar cells under different irradiances, temperatures and spectra, or the method developed in [75] to predict the maximum power of a LCPV system by considering the

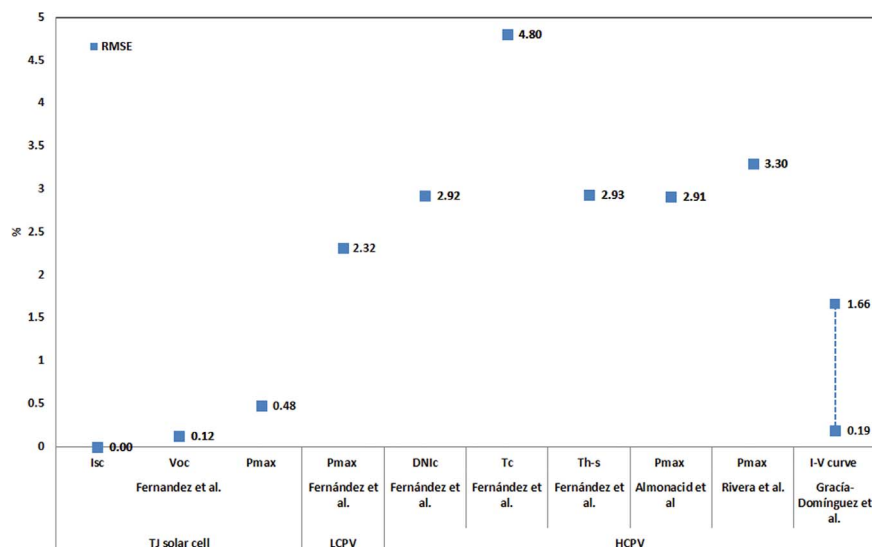


Fig. 11. RMSE values provided by each author obtained with the different methods developed for the electrical characterization of CPV devices.

transverse and longitudinal incidence angles, as well as the different components of the incident irradiance. Furthermore, the use of ANNs for modelling complex physical effects of MJ solar cells as tunnelling effects, as well as the EQE of these devices, is proved to be a powerful tool as has been shown in the studies conducted by Patra et al. [80,81,83,84]. In addition, ANNs have proved to produce a higher accuracy than other methods based on conventional analytical solutions for the modelling of HCPV modules. This is the case, for instance, of the method introduced in [86] to obtain their effective irradiance, the procedures discussed in [78,87,97] to predict their cell and/or heat-sink temperatures, the model analysed in [91,98] to predict their output power, or the methodology discussed in [95,99] to simulate their whole I-V characteristics as a function of the relevant weather variables. Fig. 11 graphically shows the RMSE values obtained with the different methods developed for the electrical characterization of CPV devices. As in the previous cases (Sections 2.1 and 2.2), this parameter has been selected to compare the different methods since is the most widely used by the various authors. As can be seen from this figure, this value is less than 5% for all ANN-based methods, which demonstrates the high accuracy and convenience of ANNs for CPV modelling applications.

4. Conclusions

In this paper, various applications of artificial neural networks (ANNs) for modelling of concentration photovoltaic (CPV) devices have been reviewed. The electrical characterization of CPV devices is a crucial task for the design, study, improvement and implementation of systems based on this technology. However, the characterization of devices based on this technology is more complex than traditional PV devices, mainly due to the use of the optical element. Furthermore, in the case of HCPV, the use of MJ solar cells increases this level of complexity. Several authors have developed ANN based models to address issues related to CPV technology. Published papers presented show the potential of the ANNs as powerful tool for modelling the CPV technology. Regarding the reviewed papers, which include the latest research work in the applications of ANNs for modelling CPV devices, the following key conclusions can be made:

- The ANNs-based models allow the electrical characterization the LCPV and HCPV devices to be done with a great level of accuracy. Furthermore, due to the fact that most of them are based on atmospheric parameters it is possible to estimate their electrical behaviour at a desired site if the atmospheric parameters are available.
- The ANNs models developed allow the cell temperature of a HCPV device to be estimated indirectly from atmospheric parameters, avoiding the need to access inside the module, and therefore damage it.
- The ANN-based models developed, offer an excellent and alternative tool for the simulation of MJ solar cells.

However, despite the fact that ANNs have been applied to solve several problems related with the CPV technology and they gave very good results, some issues related with this technology have been not covered yet. Some of these issues in which the use of ANNs could be useful, include:

- To characterise the spectrum for CPV applications.
- Electrical characterization of the new devices that are coming soon, such as MJ solar cells based in four junctions or metamorphic solar cells.
- To estimate the IV characteristic of LCPV devices.
- To estimate the effective irradiance, spectrally and angularly corrected, for LCPV devices.

Acknowledgments

This work is part of the project ENE2013-45242-R supported by the Spanish Economy Ministry, and by the European Regional Development Fund/Fondo Europeo de Desarrollo Regional (ERDF / FEDER). This work is also part of the Project “Desarrollo de un módulo fotovoltaico basado en nuevos conceptos ópticos operando a ultra alta concentración (UHCPV) ref: UJA2015/07/01” supported by the Universidad de Jaén and by the Caja Rural de Jaén.

References

- [1] Luque A, Sala G, Luque-Heredia I. Photovoltaic concentration at the onset of its commercial deployment. *Prog Photovolt: Res Appl* 2006;14(5):413–28.
- [2] Swanson RM. The promise of concentrators. *Prog Photovolt: Res Appl* 2000;8(1):93–111.
- [3] Pérez-Higueras P, Fernández EF. High concentrator photovoltaics: fundamentals, engineering and power plants. Springer; 2015.
- [4] Pérez-Higueras P, Muñoz E, Almonacid G, Vidal P. High Concentrator PhotoVoltaics efficiencies: Present status and forecast. *Renew Sustain Energy Rev* 2011;15(4):1810–5.
- [5] Chemisana D. Building Integrated Concentrating Photovoltaics: a review. *Renew Sustain Energy Rev* 2011;15:603–11.
- [6] Menoufi K, Chemisana D, Rosell J. Life cycle assessment of a building integrated concentrated photovoltaic scheme. *Appl Energy* 2013;111:505–14.
- [7] Gómez-Gil FJ, Wang X, Barnett A. Energy production of photovoltaic system: fixed, tracking and concentrating. *Renew Sustain Energy Rev* 2012;16:306–13.
- [8] Pthenakis V, Kim H. Life cycle assessment of high-concentration photovoltaic systems. *Prog Photovolt: Res Appl* 2013;21(3):379–88.
- [9] Reportlinker . Globaldata. Concentrated Photovoltaics (CPV) – Global Market Size, Competitive Landscape and Key Country Analysis to 2020. New York, U.K.: PRNewswire; 2014.
- [10] Friedman D, King R, Swanson R, McJannet J, Gwinner D. Toward 100 gigawatts of concentrator photovoltaics by 2030. *IEEE J Photovolt* 2013;3(4):1460–3.
- [11] Nishimura A, Hayashi Y, Tanaka K, Hirota M, Kato S, Ito M, Araki KHE. Life cycle assessment and evaluation of energy payback time on high-concentration photovoltaic power generation system. *Appl Energy* 2010;87(9):2797–807.
- [12] Leloux J, Lorenzo E, García-Domingo B, Aguilera J, Gueymard C. A bankable method of assessing the performance of a CPV plant. *Appl Energy* 2014;118:1–11.
- [13] Talavera D, Pérez-Higueras P, Ruiz-Arias J, Fernández E. Levelised cost of electricity in high concentrated photovoltaic grid connected systems: spatial analysis of Spain. *Appl Energy* 2015;151:49–59.
- [14] Fernández E, Talavera D, Almonacid F, Smestad G. Investigating the impact of weather variables on the energy yield and cost of energy of grid-connected solar concentrator systems. *Energy* 2016;106:790–801.
- [15] Rodrigo P, Fernández E, Almonacid F, Pérez-Higueras P. Models for the electrical characterization of high concentration photovoltaic cells and modules: a review. *Renew Sustain Energy Rev* 2013;26:752–60.
- [16] Fernández EF, Pérez-Higueras P, Almonacid F, Ruiz-Arias JA, Rodrigo P, Fernandez JI, Luque-Heredia I. Model for estimating the energy yield of a high concentrator photovoltaic system. *Energy* 2015;87:77–85.
- [17] Fernández EF, García-Loureiro A, Smestad GP. Multijunction concentrator solar cells: analysis and fundamentals. In: High concentrator photovoltaics: fundamentals, engineering and power plants. Springer; 2015. p. 9–37.
- [18] Theristis M, Fernández E, Stark C, O'Donovan T. A theoretical analysis of the impact of atmospheric parameters on the spectral, electrical and thermal performance of a concentrating III-V triple-junction solar cell. *Energy Convers Manag* 2016;117:218–27.
- [19] Fernandez EF, Almonacid F, Ruiz-Arias J, Soria-Moya A. Analysis of the spectral variations on the performance of high concentrator photovoltaic modules operating under different real climate conditions. *Sol Energy Mater Sol Cells* 2014;127:179–87.
- [20] Shanks K, Senthilarasu S, Mallick T. Optics for concentrating photovoltaics: trends, limits and opportunities for materials and design [pp. 394–407]. *Renew Sustain Energy Rev* 2016;Vols. 60:394–407, [pp. 394–407].
- [21] Rodrigo P, Fernández E, Almonacid F, Pérez-Higueras P. Review of methods for the calculation of cell temperature in high concentration photovoltaic modules for electrical characterization. *Renew Sustain Energy Rev* 2014;38:478–88.
- [22] Almonacid F, Pérez-Higueras P, Fernández E, Rodrigo P. Relation between the cell temperature of a HCPV module and atmospheric parameters. *Sol Energy Mater Sol Cells* 2012;105:322–7.
- [23] Fernández, E F, Soria-Moya, A, Almonacid, F, Aguilera, J. Comparative assessment of the spectral impact on the energy yield of high concentrator and conventional photovoltaic technology. *Solar Energy Materials and Solar Cells*, vol. 147, pp. 185–197.
- [24] Ruiz-Arias J, Quesada-Ruiz S, Fernández E, Gueymard C. Optimal combination of gridded and ground-observed solar radiation data for regional solar resource assessment [pp. 411–424]. *Sol Energy*. 112 2015;112:411–24.
- [25] Kurtz S, Muller M, Jordan D, Ghosal K, Fisher B, Verlinden P, Hashimoto J, Riley D. Key parameters in determining energy generated by CPV modules. *Prog Photovolt: Res Appl* 2015;23(10):1250–9.
- [26] Kalogirou S. Application of Artificial neural networks for energy systems. *Appl*

- Energy 2000;67:17–35.
- [27] Kalogirou S. Application of Artificial neural networks in renewable energy systems applications: a review. *Renew Sustain Energy Rev* 2001;5:373–401.
- [28] Hontoria L, Aguilera J, Riesco J, Zufiria P. Recurrent neural supervised models for generating solar radiation. *J Intell Robot Syst* 2001;31:201–21.
- [29] Hontoria L, Aguilera J, Zufiria P. Generation of hourly irradiation synthetic series using the neural network multilayer perceptron. *Sol Energy*, 2002;72(5):441–6.
- [30] Al-Alawi S, Al-Hinai H. An ANN-based approach for predicting global radiation in location with no direct measurement instrumentation. *Renew Energy*, 1998;14:199–204.
- [31] Mellit A, Benghanem M, Hadj Arab A, Guessoum A. A simplified model for generating sequences of global radiation data for insolated sites: using neural network and library of Markov transition matrices. *Sol Energy* 2005;79(5):468–82.
- [32] Mellit A, Benghanem M, Kalogirou S. An adaptive wavelet-network model for forecasting daily total solar. *Appl Energy*, 2006;83:704–22.
- [33] Bahgat A, Helwa N, Ahamd G, El Shenawy E. Estimation of the maximum power and normal operating power of a photovoltaic module by neural networks. *Renew Energy* 2004;29:443–57.
- [34] Himaya T, Katabayashi K. Neural network based estimation of maximum power generation from PV module using environmental information. *IEEE Trans Energy Convers*, 1997;12(3):241–7.
- [35] Mellit A, Benghanem M, Hadj Arab A, Guessoum A. An adaptive artificial neural network model for sizing stand-alone photovoltaic systems: application for isolated sites in Algeria. *Renew Energy*, 2005;30(10):1501–24.
- [36] Mellit A, Benghanem M, Kalogirou S. “Modelling and simulation of standalone photovoltaic system using an adaptive artificial neural network. *Renew Energy* 2007;32(2):285–313.
- [37] Veerachary M, Yadaiah N. ANN based peak power tracking for PV supplied motors. *Sol Energy* 2000;69(4):343–50.
- [38] Bahgat A, Helwa N, Ahamd G, El Shenawy E. Maximum power point tracking controller for PV systems using neural networks. *Renew Energy* 2005;30:1257–68.
- [39] Karapete E, Boztepe M, Colak M. Neural network based solar cell model. *Energy Convers Manag* 2006;47:1159–78.
- [40] de Blas M, Torres J, Prieto E, García A. Selecting a suitable model for characterizing photovoltaic devices. *Renew Energy* 2002;25:371–80.
- [41] Almonacid F, Rus C, Hontoria L, Fuentes M, Nofuentes G. Characterisation of Si-crystalline PV modules by artificial neural networks. *Renew Energy* 2009;no. 34:941–9.
- [42] Almonacid F, Rus C, Hontoria L, F.J.M. Characterisation of PV CIS module by artificial neural networks. A comparative study with other methods. *Renew Energy* 2010;35:973–80.
- [43] Almonacid F, Rus C, Pérez-Higueras P, Hontoria L. Calculation of the energy provided by a PV generator. Comparative study: conventional methods vs artificial neural networks. *Energy* 2011;36:375–84.
- [44] Almonacid F, Rus C, Pérez-Higueras P, Hontoria L. Estimation of the energy of a PV generator using artificial neural network. *Renew Energy* 2009;no. 34:2743–50.
- [45] Mellit A, Kalogirou S. Artificial intelligence techniques for photovoltaic applications: a review. *Prog Energy Comb Sci* 2008;34:574–632.
- [46] Chan N, Young TB, Brindley HE, Elkins-Daukes N, Araki K, Kemmoku YY. Validation of energy prediction method for a concentrator photovoltaic module in Toyohashi Japan. *Prog Photovolt: Reserch Appl* 2012.
- [47] Steinner M, Siefert G, Hornung T, Peharz G, Bett A. YieldOpt, a model to predict the power output and energy yield for concentrating photovoltaic modules. *Prog Photovolt: Res Appl* 2014.
- [48] Xie WT, Dai Y, Wang R, Sumathy K. Concentrated solar energy applications using Fresnel lenses: a review. *Renew Sustain Energy Rev* 2011;15(6):2588–606.
- [49] Victoria M, Domínguez C, Anón I, Sala G. Comparative analysis of different secondary optical elements for aspheric primary lenses. *Opt Express* 2009;17(9):6487–92.
- [50] Rodrigo P, Micheli L, Almonacid F. The high-concentrator photovoltaic module. In: Perez-Higueras P, Fernández P, Eduardo F, editors. *High Concentrator Photovoltaics: Fundamentals, Engineering and Power Plants*. Springer; 2015. p. 115–51.
- [51] Sarmah N, Richards B, Mallick T. Evaluation and optimization of the optical performance of low-concentrating dielectric compound parabolic concentrator using ray-tracing methods. *Appl Opt* 2011;50(19):3303–10.
- [52] Baig H, Fernandez EF, Mallick T. Influence of spectrum and latitude on the annual optical performance of a dielectric based BICPV system. *Sol Energy* 2016;124:268–77.
- [53] Mellit A. Artificial Intelligence technique for modelling and forecasting of solar radiation data: a review. *Int J Artif Intell Soft Comput* 2008;1(1):52–76.
- [54] Coimbra CF, Kleissl J, Marqu ez R. Chapter 8: overview of solar-forecasting methods and a metric for accuracy evaluation,”evaluation. In: *Solar energy forecasting and resource assessment*. Elsevier; 2013. p. 172–92.
- [55] Lopez G, Batlles F, Tovar-Pescador J. Selection of input parameters to model direct solar irradiance by using artificial neural networks. *Energy* 2005;30:1675–84.
- [56] Alam S, Kaushik S, Garg S. Computation of beam solar radiation at normal incidence using artificial neural network. *Renew Energy* 2006;31:1483–91.
- [57] Mishra A, Kaushika N, Zhang G, Zhou J. Artificial neural network model for the estimation of direct solar radiation in the Indian zone. *Int J Sustain Energy* 2008;27(3):95–103.
- [58] Mellit A, Eleuch H, Benghanem M, Elaoun C, Pavan A. An adaptive model for predicting of global, direct and diffuse hourly solar irradiance. *Energy Convers Manag* 2010;51:771–82.
- [59] Mubiru J. Using artificial neural networks to predict direct solar irradiation. *Adv Artif Neural Syst* 2011;2011:1–6.
- [60] Marquez R, Coimbra C. Forecasting of global and direct solar irradiance using stochastic learning methods, ground experiments and the NWS database. *Sol Energy* 2011;85:746–56.
- [61] J. Rodrigo, L. Hontoria, F. Almonacid, E. Fernández, P. Rodrigo and P. J. Pérez-Higueras, Artificial neural networks for the generation of direct normal solar annual irradiance synthetic series. in: *AIP Conference In: Proceedings of the 8th international conference on concentrating photovoltaic systems: CPV-8*. Toledo, Spain; 2012.
- [62] Rehman S, Mohandes M. Splitting global solar radiation into diffuse and direct normal fractions using artificial neural networks. *Energy Sources* 2012;34(14):1326–36.
- [63] Y E, Marpu P, Gherboudj I, Ghedira H, Taha BO, Chiesa M. Artificial neural network based model for retrieval of the direct normal, diffuse horizontal and global horizontal irradiances using SEVIRI images. *Sol Energy* 2013;89:1–16.
- [64] Chu Y, Pedro HT, Coimbra CF. Hybrid intra-hour DNI forecasts with sky image processing enhanced by stochastic learning. *Sol Energy* 2013;98:592–603.
- [65] Alobaidi MH, Marpu PR, Ouarda TBMJ, Ghedira H. Mapping of the solar irradiance in the UAE using advanced artificial neural network ensemble. *IEEE J Sel Top Appl Earth Obs Remote Sens* 2014;7(8):3668–80.
- [66] Renno C, Petito F, Gatto A. Artificial neural network models for predicting the solar radiation as input of a concentrating photovoltaic system. *Energy Convers Manag* 2015;106:999–1012.
- [67] Tasadduq I, Rehman S, Bubshait K. Application of neural networks for the prediction of hourly mean surface temperatures in Saudi Arabia. *Renew Energy* 2002;25:545–54.
- [68] Abdel-Aal R. Hourly temperature forecasting using abductive networks. *Eng Appl Artif Intell* 2004;17:543–56.
- [69] Smith BA, Hoogenboom G, McClendon R. Artificial neural networks for auto-mated year-round temperature prediction. *Comput Electron Agric* 2009;68:52–61.
- [70] Dombaycı  A, G lc  M. Daily means ambient temperature prediction using artificial neural network method: a case study of Turkey. *Renew Energy* 2009;34:1158–61.
- [71] Deligiorgi D, Philippopoulos K, Kouroupetroglou G. Artificial neural network based methodologies for the spatial and temporal estimation of air temperature: application in the Greater Area of Chania, Greece. *Int Conf Pattern Recognit Appl Methods* 2013.
- [72] Almonacid F, P rez-Higueras P, Rodrigo P, Hontoria L. Generation of ambient temperature hourly time series for some Spanish locations by artificial neural networks. *Renew Energy* 2013;51:285–91.
- [73] Cobaner M, Citakoglu H, Kisi O, Haktanir T. Estimation of mean monthly air temperatures in Turkey. *Comput Electron Agric* 2014;109:71–9.
- [74] Kisi O, Shiri J. Prediction of long-term monthly air temperature using geographical inputs. *Int J Clim* 2014;34:179–86.
- [75] Fern ndez EF, Almonacid F, Sharma N, Rodrigo P, Mallik T, P rez-Higueras P. A model based on artificial neuronal network for the prediction of the maximum power of a low concentration photovoltaic module for building integration. *Sol Energy* 2014;100:148–58.
- [76] Zahedi A. Review of modelling details in relation to low-concentration solar concentrating photovoltaic. *Renew Sustain Energy Rev* 2011;15(3):1609–14.
- [77] Fern ndez EF, P rez-Higueras P, Garcia Loureiro A, Vidal P. Outdoor evaluation of concentrator photovoltaic systems modules from different manufacturers: first results and steps. *Prog Photovolt: Res Appl* 2013;21(4):693–701.
- [78] Fern ndez EF, Almonacid F, Rodrigo P, P rez-Higueras P. Calculation of the cell temperature of a high concentrator photovoltaic (HCPV) module: a study and comparison of different methods. *Sol Energy Mater Sol Cells* 2014;121:144–51.
- [79] Fern ndez EF, Siefert G, Almonacid F, Garcia Loureiro AJ, P rez-Higueras P. A two subcell equivalent solar cell model for III–V triple junction solar cells under spectrum and temperature variations. *Sol Energy* 2013;92:221–9.
- [80] J. Patra and D. Maskell, Estimation of Dual-Junction solar cell characteristic using neural networks, In: *Proceedings of the 35th IEEE photovoltaic specialists conference, PVSC 2010*. Honolulu, HI, United States; 2010.
- [81] Patra J. Neural network-based model for dual-junction solar cells. *Prog Photovolt: Ressearch Appl* 2011;19:33–44.
- [82] SILVACO, SILVACO, [Online]. Available: (http://www.silvaco.com/products/tcad/device_simulation/atlas/atlas.html).
- [83] Patra J. Chebyshev Neural network-based model for dual-junction solar cells. *IEEE Trans Energy Convers*, 2011;26(1):132–9.
- [84] Patra J, Maskell D. Modeling of multi-junction solar cells for estimation of EQE under influence of charged particles using artificial neural networks. *Renew Energy* 2012;44:7–16.
- [85] Fern ndez EF, Almonacid F, Gracia-Loureiro A. Multi-junction solar cells electrical characterization by neuronal networks under different irradiance, spectrum and cell temperature. *Energy*, 2015;90:846–56.
- [86] Fern ndez E, Almonacid F. Spectrally corrected direct normal irradiance based on artificial neural networks for high concentrator photovoltaic applications. *Energy* 2014;74:941–9.
- [87] Fern ndez EF, Almonacid F. A new procedure for estimating the cell temperature of a high concentrator photovoltaic grid connected system based on atmospheric parameters. *Energy Convers Manag* 2015;103:1031–9.
- [88] I. Ant n, M. Mart nez, F. Rubio, R. N fiez, R. Herrero, C. Dom nguez, M. Victoria, S. Askins and G. Sala, Power rating of CPV systems based on spectrally corrected DNI. *AIP Conference Proceedings*; 2012: vol. 1477: 331–335.
- [89] King DL, Boyson WE, Kratochvil JA. Sandia National Laboratories. Photovoltaic array performance model SAND2004-3535. New Mexico, USA: Albuquerque; 2004.
- [90] Almonacid F, Mellit A, Kalogirou S. Applications of ANNs in the Field of the HCPV Technology. In: *High Concentrator Photovoltaics: Fundamentals, Engineering and*

- Power Plants. Springer; 2015. p. 333–51.
- [91] Almonacid F, Fernández EF, Rodrigo P, Pérez-Higueras P, Rus-Casas C. Estimating the maximum power of a High Concentrator Photovoltaic (HCPV) module using an Artificial Neural Network. *Energy* 2013;53:165–72.
- [92] Rivera A, García-Domingo B, Del Jesus M, Aguilera J. Characterization of concentrating Photovoltaic modules by cooperative competitive radial basis function networks. *Expert Syst Appl* 2013;40(5):1599–608.
- [93] S. Williams, T. Betts, T. Helf, R. Gottschalg, H. Beyer and D. Infield, Modeling long term module performance based on realistic reporting conditions with consideration to spectral effects., in: *Proceedings of the world conference on photovoltaic energy conversion*; 2003.
- [94] Takashi M, Yasuhito N, Hiroaki T, Hideyuki T. Uniqueness verification of solar spectrum index of average photon energy for evaluating outdoor performance of photovoltaic modules. *Sol Energy* 2009;83:1294–9.
- [95] Almonacid F, Fernández EF, Mallick T, Pérez-Higueras P. High concentrator photovoltaic module simulation by neuronal networks using spectrally corrected direct normal irradiance and cell temperature. *Energy*, 2015;84:336–43.
- [96] García-Domingo B, Piliouguine M, Elizondo D, Aguilera J. CPV module electric characterisation by artificial neural networks. *Renew Energy* 2015;78:173–81.
- [97] E. F. Fernández, F. Almonacid, L. Micheli and T. Mallick, Comparison of methods for estimating the solar cell temperature and their influence in the calculation of the electrical parameters in a HCPV module, *AIP Conference Proceedings*; 2014: vol. 1616: 183–186.
- [98] Soria-Moya A, Almonacid Cruz F, Fernandez E, Rodrigo P, Mallick T, Perez-Higueras P. Performance Analysis of models for calculating the maximum power of high concentrator photovoltaic modules. *IEEE J Photovolt* 2015;5(3):947–55.
- [99] Almonacid F, Rodrigo P, Fernández E. Determination of the current-voltage characteristics of concentrator systems by using different adapted conventional techniques. *Energy* 2016;101:146–60.